Remote Sensing Applications: Society and Environment 37 (2025) 101499

Contents lists available at ScienceDirect

Remote Sensing Applications: Society and Environment

journal homepage: www.elsevier.com/locate/rsase

Integrating process-based vegetation modelling with high-resolution imagery to assess bark beetle infestation and land surface temperature effects on forest net primary productivity

Haidi Abdullah [a,*], Elnaz Neinavaz [a], Roshanak Darvishzadeh [a], Margarita Huesca [a], Andrew K. Skidmore [a], Mats Lindeskog [b], Benjamin Smith [b,c], Marco Heurich [d,e,f], Rainer Steinbrecher [g], Marc Paganini [h]

[a] Department of Natural Resources Science, Faculty of Geo-Information Science and Earth Observation (ITC), University of Twente, Hallenweg 8, 7522 NH, Enschede, the Netherlands
[b] Department of Physical Geography and Ecosystem Science, Lund University, Sölvegatan 12, Lund SE-223 62, Sweden
[c] Hawkesbury Institute for the Environment, Western Sydney University, Penrith, NSW, Australia
[d] Department of National Park Monitoring and Animal Management, Bavarian Forest National Park, Freyunger Str. 2, Grafenau, 94481, Germany
[e] Faculty of Environment and Natural Resources, University of Freiburg, Tennenbacher Straße 4, 79106, Freiburg im Breisgau, Germany
[f] Department of Forestry and Wildlife Management, Campus Evenstad, Inland Norway University of Applied Sciences, Postboks 400 Vestad, 2418, Elverum, Norway
[g] Karlsruhe Institute of Technology KIT, Institute of Meteorology and Climate Research, Atmospheric Environmental Research (IMK-IFU), Kreuzeckbahn Straße 19, Garmisch-Partenkirchen, 82467, Germany
[h] European Space Research Institute (ESRIN), European Space Agency, Frascati, Italy

ARTICLE INFO

Keywords:
Net primary productivity
LPJ-GUESS
Sentinel-2
Bark beetle infestation
Leaf area index
Land surface temperature
Climate change

ABSTRACT

The European spruce bark beetle (*Ips typographus*) is an insect species that causes significant damage to Norway spruce (*Picea abies*) forests across Europe. Infestation by bark beetles can profoundly impact forest ecosystems, affecting their structure and composition and affecting the carbon cycle and biodiversity, including a decrease in net primary productivity (NPP), a key indicator of forest health. The primary objective of this study is to enhance our understanding of the interplay among NPP, bark beetle infestation, land surface temperature (LST), and soil moisture content as key components influencing the effects of climate change-related events (e.g., drought) during and after a drought event in the Bavarian Forest National Park in southeastern Germany. Earth observation data, specifically Landsat-8 TIR and Sentinel-2, were used to retrieve LST and leaf area index (LAI), respectively. Furthermore, for the first time, we incorporated a time series of high-resolution (20 m) LAI as a remote sensing biodiversity product into a process-based ecological model (LPJ-GUESS) to accurately generate high-resolution (20 m) NPP products. The study found a gradual decline in NPP values over time due to drought, increased LST, low precipitation, and a high rate of bark beetle infestation. We observed significantly lower LST in healthy Norway spruce stands compared to those infested by bark beetles. Likewise, low soil moisture content was associated with minimal NPP value. Our results suggest synergistic effects between bark beetle infestations and elevated LST, leading to amplified reductions in NPP value. This study highlights the critical role of integrating high-resolution remote sensing data with

* Corresponding author. Faculty of Geo-Information Science and Earth Observation (ITC), University of Twente, PO Box 217, Drienerlolaan 5, 7500 AE, Enschede, the Netherlands.
E-mail address: H.j.abdullah-1@utwente.nl (H. Abdullah).

https://doi.org/10.1016/j.rsase.2025.101499
Received 13 November 2024; Received in revised form 13 February 2025; Accepted 20 February 2025
Available online 24 February 2025

ecological models for advancing the understanding of forest carbon dynamics and improving predictive capabilities to inform forest management under climate change.

1. Introduction

The European spruce bark beetle (*Ips typographus*) is an insect herbivore primarily targeting mature and old Norway spruce (*Picea abies*) stands, causing widespread outbreaks across European coniferous forests (Fahse and Heurich, 2011; Müller et al., 2008; Senf and Seidl, 2021). Bark beetle infestations can spread rapidly under favourable climatic and forest stand conditions (Christiansen and Bakke, 1988; Seidl et al., 2016). Climate change exacerbates these outbreaks, as higher temperatures lead to earlier hatching and faster development of beetles (Wermelinger, 2004), with severe infestations fuelled by rising temperatures and extreme drought events (Pirtskhalava-Karpova et al., 2024). Droughts weaken trees by reducing resin production, a primary defence against beetles, making them more vulnerable (Wermelinger, 2004). These outbreaks have significantly altered European forest ecosystems, reducing timber production, impacting tourism, and resulting in substantial economic losses. For instance, approximately 360 million m^3 of Norway spruce timber was destroyed between 2018 and 2021 (Melegari, 2022) .

One critical consequence of bark beetle infestations is the disruption of forest ecosystems, affecting their structure, composition, carbon cycling and biodiversity (Pfeifer et al., 2011; Seidl et al., 2014; Zeppenfeld et al., 2015). Tree mortality and reduced stand density release stored carbon through changes in decomposition and respiration rates (Hlásny et al., 2021). This highlights the importance of considering bark beetle dynamics in policies designed to enhance forest carbon sequestration (Beudert and Gietl, 2015; Seidl et al., 2008). Bark beetle-induced tree mortality also reduces Net Primary Productivity (NPP), i.e. the balance between photosynthesis and respiration, which is the primary pathway of carbon into plants and ecosystems and is therefore a critical indicator of forest health (Ainsworth et al., 2012). Reduced NPP can result from various factors, including reduced light, water, or nutrient availability, as well as forest dieback, which represents a more extreme scenario. These changes directly influence ecosystem management strategies and biodiversity conservation (Crabtree et al., 2009; Xiao et al., 2003). Its significance has led to its recognition as an 'Essential Biodiversity Variable' (EBV) to be monitored via Earth Observation (EO) (Pereira et al., 2013; Skidmore et al., 2021).

The link between bark beetle infestations, NPP, and climate parameters is complex and intertwined. NPP is directly influenced by photosynthesis, which depends on climatic factors such as temperature, soil moisture, and solar radiation. Rising temperatures, especially as reported in the mountainous region of Central Europe (Böhm et al., 2001), are a key driver of bark beetle outbreaks, as warmer habitat conditions can initially boost photosynthesis up to a species-specific optimum (Berry and Bjorkman, 1980). However, prolonged heat stress or extreme temperatures suppress photosynthesis and NPP by disrupting enzymatic activities and increasing respiration rates (Das et al., 2023). Similarly, soil moisture content—a vital factor for plant water uptake and nutrient transport—affects NPP through its role in photosynthesis regulation. Drought-induced low soil moisture limits stomatal conductance, decreasing CO_2 uptake, which reduces photosynthesis and, consequently, NPP (Kramer and Boyer, 1995). Prolonged drought can also cause xylem embolism, further impairing plant productivity and health (Ghalambor et al., 2007).

Moreover, bark beetle outbreaks disrupt canopy structure, increasing Land Surface Temperature (LST) and altering soil moisture dynamics (Tait and Schiel, 2013). These changes, in turn, profoundly affect NPP. For instance, as bark beetles kill stands of Norway spruce, they break the natural canopy cover, exposing more ground to sunlight. This exposure elevates LST by increasing the absorption of solar radiation and reducing the cooling effect provided by evapotranspiration (Putuhena and Cordery, 2000; Tomes et al., 2024). Although reduced evapotranspiration can initially lead to higher soil moisture content in certain areas, the loss of canopy shading and insulation ultimately amplifies temperature fluctuations, potentially causing localized drying under prolonged heat or drought conditions.

Elevated LST may temporarily enhance photosynthetic rates, but prolonged exposure to high temperatures can lead to overheating, reducing photosynthetic efficiency and increasing stress on trees (Tait and Schiel, 2013). Consequently, these shifts in soil moisture dynamics and canopy loss exacerbate drought conditions, compounding their adverse effects on NPP. This highlights the critical interplay between LST and soil moisture in shaping forest resilience. Abundant soil moisture can moderate temperature extremes through evaporative cooling, mitigating plant heat stress and reducing the cascading impacts of bark beetle infestations (Cooper et al., 2017; Yue et al., 2022).

Recent trends of increasing temperatures and frequent heatwaves in Europe (Semenza and Paz, 2021; Yin et al., 2024) amplify dynamics of the kind described above. Warmer conditions accelerate bark beetle life cycles (Marini et al., 2017; Wermelinger, 2004) and simultaneously create feedback loops that reduce forest NPP. For example, drought-induced water stress weakens trees, increasing their susceptibility to beetles while also reducing their carbon fixation capacity.

Understanding the complex dynamics between bark beetle outbreaks, climate parameters (e.g., LST), and NPP highlights the necessity of robust tools to effectively monitor and model these interactions. While conventional metrics, such as satellite-derived products like MODIS NPP, provide valuable insights at broader scales, they often lack the granularity required to capture localized forest disturbances and their impacts on ecosystem processes. This gap highlights the importance of integrating high-resolution EO data with modeling to generate precise, spatially detailed NPP estimates.

Models that simulate tree and forest growth can help us understand how climate and soil conditions influence tree health, structure, and survival (Fisher et al., 2018; Medvigy et al., 2009). These models are useful for identifying how forest disturbances (e.g., bark beetle outbreaks) lead to losses in forest productivity by illustrating the key steps in this process (Seidl et al., 2017). Therefore, more advanced methods are needed to unravel the complex connections between bark beetle infestations, soil moisture, and LST, especially

as climate change makes these interactions more unpredictable (Anderegg et al., 2020).

Numerous products are available that estimate NPP in forested ecosystems from spectral reflectance data from satellites, the MODIS-NPP product being among the most widely used. The MODIS imagery provides global NPP estimates by integrating EO data with models incorporating vegetation type, temperature, and precipitation (Running and Zhao, 2015). However, its coarse resolution of 1 km limits the suitability of the MODIS product for local-scale investigations. Process-based climate-vegetation models, such as LPJ-GUESS, simulate carbon and water cycling in ecosystems based on vegetation dynamics and inputs like temperature, precipitation, soil properties, and land use (Lindeskog et al., 2021; Smith et al., 2001). The model has been used to simulate bark beetle impacts under climate change (Jönsson et al., 2015), but is constrained in normal application by a typical grid resolution of 10–50 km, limiting utility for fine-scale studies. This study enhances LPJ-GUESS outputs by rescaling them using satellite data, generating high-resolution NPP products at 20 m resolution (method section 2.3). Using a leaf area index (LAI) product generated from Sentinel-2, this Satellite-Enhanced NPP Product enables finer analysis of forest disturbances, such as bark beetle infestations, and explores interactions with other EO indicators like LST, as a proxy for extreme climate events (e.g., drought and heatwaves) (Anderegg et al., 2020; Seidl et al., 2017; Yue et al., 2022).

The primary objective of this study is to investigate the intricate interactions between bark beetle infestations and LST and their combined influence on NPP. This research specifically aims to enhance our understanding of how LST and bark beetle infestations collectively influenced NPP dynamics in the Bavarian Forest National Park, Germany, from 2016 to 2020. Additionally, it investigates the role of soil moisture content in mediating these interactions. We design a novel method for leveraging high-resolution NPP data obtained by modifying the physical LPJ-GUESS model with high-resolution EO data, in order to explain and clarify the complex relationships between soil moisture content, LST, and NPP.

2. Materials and methods

2.1. Study area

The Bavarian Forest National Park (hereafter BFNP), located in southeastern Germany, along the border with the Czech Republic (49°3′19″ N and 13°12′9″ E), forms a part of the expansive Bohemian Forest (Fig. 1). This is the largest continuously protected forest area in central Europe and comprises three interconnected parts: Šumava in the Czech Republic, BFNP in Germany, and Raumeinheit Böhmerwald in Austria (Abdullah et al., 2018a; König et al., 2023). The climate within BFNP is classified as temperate. It experiences an annual precipitation range of 900 mm–1800 mm. The region contains diverse elevational gradients, ranging from 600 m to 1450 m above sea level. The area can be categorized into three distinct ecological zones based on elevation and species composition. The high elevation zone, situated above approximately 1100–1200 m a.s.l., is dominated by spruce, which accounts for 90% of the tree species in this zone, with a smaller proportion of European beech (*Fagus sylvatica*) and mountain ash (*Sorbus aucuparia*) also present. Below this altitude (i.e., 900–1100 a.s.l), the hillsides form the second zone, representing a mixed montane forest. This zone is primarily occupied by Norway spruce (approximately 58%), with the remainder comprising a blend of European silver fir (*Abies alba*) and European beech (*Fagus sylvatica*). The valley bottoms, constituting the third ecological zone, are also predominantly dominated (83%) by Norway spruce, with the remaining portion consisting of mixed stands of other species (Beudert and Gietl, 2015; Heurich et al., 2010). The

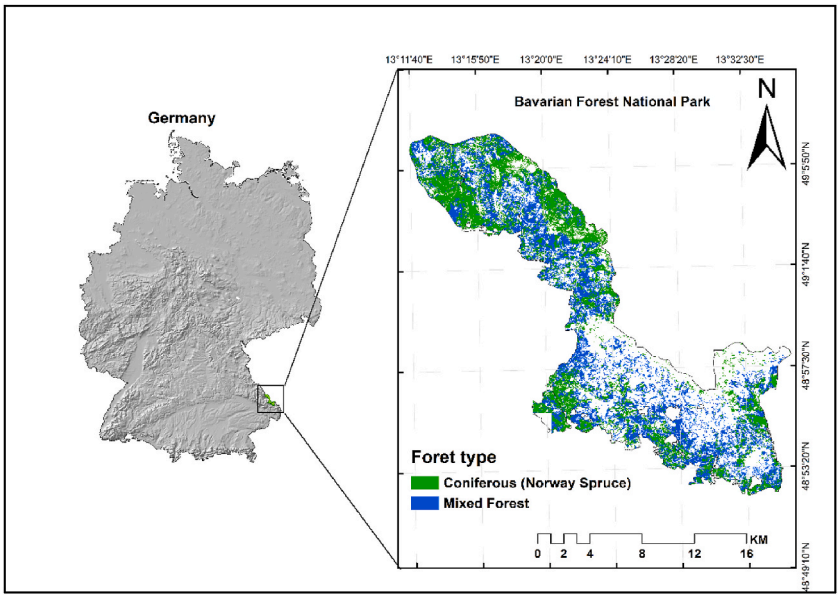

Fig. 1. The location of the Bavarian Forest National Park in Germany and the distribution of coniferous and mixed forest stands (Latifi et al., 2021).

infestations of bark beetles that began in 1984 have caused significant disturbances in the BFNP (König et al., 2023). The BFNP management includes a 75% non-intervention zone, prohibiting forest and wildlife management. Along the park's edges, in the management zone, bark beetle control is implemented to prevent its spread to neighbouring forests.

2.2. Data

Fig. 2 provides an overview of the workflow used in this study for calculating NPP and LST. The workflow integrates various datasets and processing steps, which are elaborated on in the following sub-sections.

2.2.1. Field data

Field data were collected during the summers of 2015 (n = 31) and 2016 (n = 21) using stratified random sampling to represent the major cover types. Representative sample plots, each covering an area of approximately 900 m^2 (30 m × 30 m), were selected. The precise locations of these plots were recorded with a Leica GPS 1200 (Leica Geosystems AG, Heerbrugg, Switzerland), achieving a post-processed positioning accuracy of less than 1 m.

Within each plot, LAI was measured using a LI-COR LAI-2200 canopy analyzer (LI-COR, 1992). For each plot, three above-canopy observations were taken in nearby forest openings to minimize variability in incoming radiation. Subsequently, five below-canopy LAI observations were collected within each plot. The average of these below-canopy observations was used to represent the plot's LAI (Gara et al., 2019). To ensure accuracy, consistent illumination conditions were maintained during both above- and below-canopy readings. These in-situ LAI measurements were further utilized to estimate LAI at a 20 m resolution and to enhance the spatial resolution of the NPP product derived from the LPJ-GUESS model (Sections 2.2.2.2 and 2.).

2.2.2. Remote sensing data and processing

To achieve the study's objective of investigating the interactions among bark beetle infestation, LST, soil moisture content, and NPP, various EO datasets and products were utilized. LST was derived from the thermal band of Landsat-8, while LAI was calculated using Sentinel-2 data. The calculated LAI was then integrated into the LPJ-GUESS model to enhance the spatial resolution of the NPP product. The workflow for calculating LST and improving the NPP spatial resolution is presented in Fig. 2 and is detailed in the following subsections.

2.2.2.1. Calculating land surface temperature. LST was calculated using the thermal infrared band 10 of Landsat-8, which detects wavelengths in the range of 10.60 μm–11.19 μm. While Landsat-8's thermal bands are originally collected at a 100 m spatial

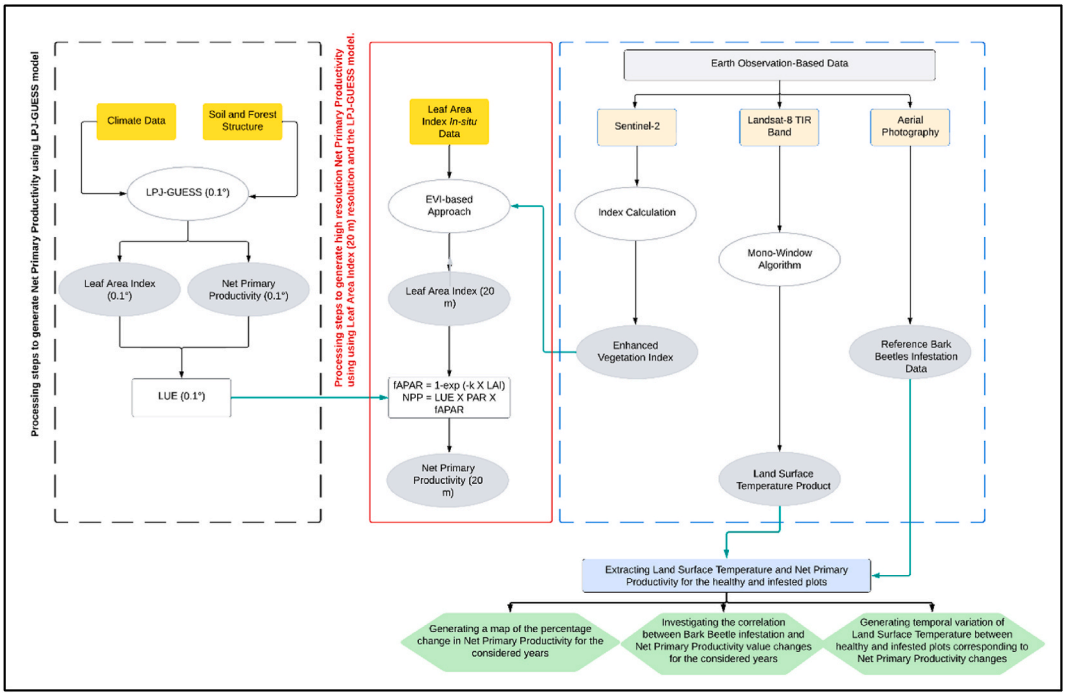

Fig. 2. An approach for calculating Earth observation-adjusted Net Primary Productivity (NPP) by integrating LPJ-GUESS modelled NPP with Leaf Area Index (LAI) derived using 20-m resolution Sentinel-2 imagery. LAI, LUE (Light Use Efficiency), EVI (Enhanced Vegetation Index), fAPAR (Fraction of Absorbed Photosynthetically Active Radiation), and PAR (Photosynthetically Active Radiation) are included. FPAR is calculated using the modelled LAI from Sentinel2.

resolution, they are resampled and provided at 30 m resolution to ensure consistency with other Landsat-8 bands in the visible and shortwave infrared regions (Abdullah et al., 2020b; Neinavaz et al., 2019). To align the LST data with NPP, which we generated at a 20 m spatial resolution (see section 2.3), we further resampled the 30 m LST data to 20 m using bilinear interpolation.

A common approach for determining LST involves converting top-of-atmosphere (TOA) spectral radiance to brightness temperature. However, this method often neglects the influence of climatic conditions and geographical variability, which can significantly impact LST accuracy. Specifically, atmospheric variability affects thermal radiation transmission, while emissivity variations across different surfaces further complicate the LST retrieval process. These factors are particularly important as they influence local climate and surface temperature patterns. To address these limitations, advanced techniques incorporating atmospheric correction algorithms, emissivity estimation, and terrain correction procedures are essential for improving LST reliability.

To overcome these limitations, we employed the Mono-Window Algorithm (MWA) proposed by Qin et al. (2001). The MWA mitigates atmospheric and emissivity-related effects by integrating auxiliary data along with the thermal infrared band. These auxiliary inputs include:

- Surface emissivity, which was computed using a Normalized Difference Vegetation Index (NDVI)-based approach derived from Landsat data,
- Air transmittance and effective mean atmospheric temperature are estimated using surface air temperature and water vapor content obtained and calculated from metrological station data.
- Water vapor content itself was derived from the ratio of relative humidity to surface air temperature.

Comprehensive details regarding implementing the MWA using Landsat-8's thermal infrared band can be found in our earlier work (Abdullah et al., 2019b). For this study, thermal infrared data were collected exclusively during cloud-free conditions in August across all five years under consideration. This ensured consistency and comparability in the LST estimation process.

2.2.2.2. Calculating leaf area index. The LAI was the primary input used to enhance the spatial resolution of the NPP product generated by the LPJ-GUESS model in this study. LAI, defined as the ratio of one-sided leaf area to ground area (Chen and Black, 1992), is a critical parameter for understanding plant growth and ecosystem productivity. By directly influencing the amount of light plants can absorb and the surface area for stomatal conductance, which creates the xylem tension to draw soil resources (water and nutrients) into the plant, LAI is closely tied to NPP. As a proxy for the energy available to primary consumers in an ecosystem, LAI serves as a key indicator of forest health and productivity.

In this study, LAI was estimated at a 20 m spatial resolution using an Enhanced Vegetation Index (EVI)-based approach derived from Sentinel-2 data. The EVI-based approach has been widely and successfully applied to retrieve LAI at a global scale using MODIS data (Boegh et al., 2002). Accordingly, a similar approach was adapted in this study to generate LAI from the high-resolution Sentinel-2 dataset. To do this, EVI was computed using Sentinel-2 imagery, applying spectral bands B2 (0.490 μm), B4 (0.665 μm) and B8 (0.842 μm) as follows:

$$EVI = 2.5 * (B8 - B4) / ((B8 + 6.0 * B4 - 7.5 * B2) + 1.0) \quad \text{(Eq.1)}$$

The relationship between EVI and in situ LAI data collected over two consecutive years (2015 and 2016) (see Section 2.2.1) was then investigated, and a linear model was developed as outlined below:

$$LAI = 4.0543 *(EVI) + 1.7901 \quad \text{(Eq.2)}$$

Finally, the validation of the LAI products was performed using a cross-validation procedure (leave-one-out method). The cross-validated coefficient of determination (R^2cv) and the root mean square error (RMSE cv) between measured and estimated LAI were calculated to assess the accuracy of the LAI modelling. The developed model was subsequently used to estimate the LAI for the study site during the summer period from 2016 to 2020.

2.3. Calculating net primary productivity at high spatial resolution

To assess forest productivity in the BFNP during 2016–2020, we utilized the vegetation model LPJ-GUESS, v4.1 (Lindeskog et al., 2021; Smith et al., 2001). Although LPJ-GUESS simulates detailed biogeochemical processes, our focus was on developing a methodology to produce high-resolution gridded maps of NPP at a 20 m spatial resolution. This was achieved by integrating the Sentinel-2-derived LAI (Section 2.2.2.2) with a relationship between leaf area and productivity emerging from LPJ-GUESS simulations, following a stepwise workflow, as described below.

The process of simulating NPP using LPJ-GUESS was conducted at a spatial resolution of ~1.1 km, utilizing essential inputs such as local climate data (e.g., temperature, precipitation, and shortwave radiation), soil structure, nitrogen deposition, and atmospheric CO_2 concentration. Key datasets included bias-corrected CRU-JRA v2.2 data, local climate observations (2016–2020) from the German Weather Service (Deutscher Wetterdienst, DWD), the EFI European Tree Species Map, and the European LUCAS Topsoil database. Tree species distributions were interpolated to ~1.1 km resolution using bilinear interpolation. Further information on the datasets and processing steps can be found in Section 2.4.

The simulations used a selection of global plant functional types (PFTs) in competing mixed stands, representing key species: boreal needle leaf evergreen (BNE, e.g., *Picea abies*, *Abies alba*), boreal intermediate shade-tolerant needle leaf evergreen (BINE, e.g., *Pinus*

sylvestris), boreal needle leaf summer-green (BNS, e.g., *Larix decidua*), temperate broadleaf summer green (TeBS, e.g., *Fagus sylvatica*), and shade-intolerant broadleaf summer green (IBS, e.g., *Betula pubescens*), as well as cool-climate C3 grass.

LPJ-GUESS model outputs included monthly NPP and LAI at ~1.1 km spatial resolution, serving as the basis for the next stage: downscaling to high resolution.

Next, Sentinel-2-derived LAI products were generated using an EVI-based approach to capture spatial heterogeneity in vegetation density. These high-resolution LAI data at 20 m resolution provided the means to bridge the gap between the relatively coarse-scale results from LPJ-GUESS with the finer detail offered by Sentinel-2 imagery and produce NPP surfaces at the native resolution of the satellite imagery.

Satellite-derived Fraction of Absorbed Photosynthetically Active Radiation ($fAPAR_{sat}$) was derived from satellite-derived LAI using Beer's law of light extinction in a leaf canopy (Eq. (3)). Beer's law describes the dependency of fAPAR on light attenuation in the profile of the canopy affected by LAI

$$fAPAR = 1 - exp(-K \times LAI) \quad \text{(Eq.3)}$$

where k is an extinction coefficient, which in this study is considered as 0.5 (Sitch et al., 2003), as a typical value for European forests.

$fAPAR_{sat}$ was then used to adjust the model-derived NPP by using the model-derived $[LUE * PAR]_{mod}$ product (Eq. (4))

$$NPP_{adj=}[LUE \times PAR]_{mod} \times fAPAR_{sat} \quad \text{(Eq.4)}$$

where the [LUE * PAR]mod product was estimated from model-derived NPP and LAI for each month using Eq. (3), Eq. (5), and Eq. (6). PAR was derived from climate data (radiation) and interpolated from the model output 0.01° resolution to a 20m resolution using an inverse distance-weighted method.

$$NPP = [LUE \times APAR] \quad \text{(Eq.5)}$$

$$APAR = PAR \times fAPAR \quad \text{(Eq.6)}$$

where PAR is the photosynthetically active radiation flux incident and top of the canopy, and fAPAR is the fraction of this flux absorbed by the vegetation canopy.

This method is based on two assumptions: that the model is better at predicting LUE than at correctly representing LAI in forest stands and that the [LUE * PAR] product computed at a course climate input resolution varies less in space than the density of forest canopies, which is assumed to be accurately captured by the satellite products at fine resolution. In addition, this method of linking satellite-based estimates of canopy light absorption to the emergent relationship between canopy leaf area and NPP was previously trialled and demonstrated for the estimation of NPP of northern European conifer forests by Smith et al. (2008).

2.4. Auxiliary data

This study utilized multiple datasets, including forest land cover, bark beetle infestation data, soil moisture content, precipitation, air temperature, vegetation type, and soil properties. The forest land cover and bark beetle infestation data were obtained from the Data Pool of the Bohemian Forest Ecosystem (Latifi et al., 2021). Since the European spruce bark beetle (*Ips typographus*) exclusively targets Norway spruce (*Picea abies*), a land cover map was used to exclude non-Norway spruce stands (see Fig. 1).

Soil moisture content data were sourced from NASA's meteorological research platform (https://power.larc.nasa.gov/data-access-viewer/), with monthly data spanning the years 2016–2020. Only data from May to August were used, as these months are critical for bark beetle infestation (Abdullah et al., 2019). Similarly, mean monthly precipitation and temperature data at a ~1.1 km spatial resolution were obtained from the German Weather Service (Deutscher Wetterdienst, DWD, (https://opendata.dwd.de/climate_environment/CDC/grids_germany/). These weather parameters were used to bias-correct daily CRU-JRA v2.2 data and were collected through a combination of manual and automated measurements, supplemented by satellite data and numerical weather prediction models. Additional model inputs included shortwave radiation data from CRU-JRA v2.2, monthly nitrogen deposition data at ~55 km resolution, and CO2 data obtained from the Global Carbon Project.

Soil properties data were sourced from the European LUCAS Topsoil dataset, which provides harmonized information on the

Table 1
The auxiliary data used in the LPJ-GUESS model to calculate and enhance the spatial resolution of net primary productivity. All datasets with spatial resolutions differing from 20 m were resampled to 20 m to ensure consistency in the analysis.

Dataset	Type of data	Spatial extent	Temporal extent	Reference
Leaf area index	EO data	20 m	2016–2020	Generated in this work
**Meteo data	EO data	1 km	2016–2020	https://opendata.dwd.de
Daily Climate	Auxiliary	~55 km	1901–2020	CRU-JRA
Tree Species Data - EFI	EO data	1 km		https://efi.int/knowledge/maps/treespecies
Soil structure	Auxiliary	~1.1 km	–	European LUCAS topsoil database

* within a 20 × 20 m plot size.
** Including monthly precipitation and temperature.

physical and chemical parameters of topsoil across Europe (Ballabio et al., 2019). For this study, the latest LUCAS dataset from 2018, which consists of point-based topsoil measurements, was interpolated using Universal Kriging to generate 20 m resolution maps. This method accounts for spatial trends in the data, incorporating factors such as elevation and climate along with spatial correlation. The tree species composition was based on the EFI European Tree Species Map at 1 × 1 km resolution, which was bilinearly interpolated to ~1.1 km spatial resolution (Table 1). A selection of global plant functional types (PFTs) was used to represent competing mixed stands: boreal needleleaf evergreen (BNE) for *Picea abies* and *Abies alba*, boreal intermediate shade-tolerant needleleaf evergreen (BINE) for *Pinus sylvestris*, boreal needleleaf summer-green (BNS) for *Larix decidua*, temperate broadleaf summer green (TeBS) for *Fagus sylvatica*, and intolerant broadleaf summer green (IBS) for *Betula pubescens*.

2.5. Reference and preprocessing of bark beetle infestation data

The bark beetle infestation data has been systematically documented in the BFNP through annual airborne colour-infrared (CIR) aerial image campaigns since 1988. These aerial surveys, conducted twice a year (June–July and September–October), capture high-resolution images with a geometric resolution of 20 cm, generating approximately 147 gigabytes of data per flight. The first campaign (June–July) is conducted before visible bark beetle infestation symptoms appear, enabling the detection of newly accumulated deadwood from the previous year. The second campaign (September–October) allows for the identification of infested trees that exhibit visible signs of damage. Further information on the technical aspects of the aerial survey in the BFNP, as well as details concerning the full process of how infested patches are identified using aerial photography data in the BFNP, can be found in (Heurich et al., 2013; Latifi et al., 2021).

In this study, incorporating the reference infestation data into the analysis pipeline required initial preprocessing steps. Infested patches (polygons) smaller than 20 × 20 m were removed. As mentioned earlier, areas of infestation were manually delineated using a threshold approach, requiring at least five infested trees per patch. This criterion was applied to exclude smaller patches that do not cover a 20 × 20 m area. This decision ensured comparability and alignment with other datasets used in this study, such as LST data, which was resampled to a spatial resolution of 20 m to match the resolution of the Net Primary Productivity (NPP) data. The reference infestation data were subsequently transformed from polygon to raster format with a 20 m resolution, following a similar approach proposed in a previous study (Abdullah et al., 2019a).

2.6. Analysis of net primary productivity (NPP) and associated factors

We utilized a combination of spatial and statistical methods to assess the impact of bark beetle infestation on NPP. A pixel-wise subtraction approach was applied to generate a percentage change map illustrating the variation in NPP values between different years. This analysis specifically focused on the influence of bark beetle infestation on NPP dynamics. The 2016 NPP data, which recorded the highest values during the study period, served as reference (100%). The percentage change in NPP for subsequent years (2017, 2018, 2019, and 2020) was calculated using the following equation:

*NPP percentage change map = [((NPPy- R) / R) * 100]* (Eq.7)

Where NPP_y is the generated NPP product for the years (y = 2017, 2018, 2019 and 2020), while R is the generated NPP product for the reference year 2016.

The resulting maps highlighted regions experiencing either an increase or decrease in NPP, providing insight into how bark beetle infestations influenced productivity over time.

To further understand these dynamics, a temporal line chart was employed to visualize variations in NPP and LST values for both healthy and infested forest stands over the five years of the study. NPP and LST data were extracted from infested stands and compared with data from 500 randomly selected points in healthy stands across the Bavarian Forest National Park (BFNP), excluding areas affected by infestations. For temporal analysis, the 2016 locations of infested stands were used to extract NPP and LST values for subsequent years, enabling the generation of percentage change maps for NPP during and after bark beetle outbreaks.

Statistical analysis included a one-way ANOVA to determine significant differences in NPP and LST values between healthy and infested stands, with a significance level of $p \leq 0.05$. To explore correlations between bark beetle infestation and NPP changes, the Pearson correlation coefficient was calculated between the total infested area (in hectares) per year and the mean NPP value for the entire BFNP, encompassing both healthy and infested stands. This analysis provided insights into the relationship between infestation dynamics and changes in forest productivity.

Additionally, the role of soil moisture content in bark beetle outbreaks was examined through a comparative analysis. The mean soil moisture levels for critical months were compared with the total annual area infested by bark beetles. Both soil moisture content and infested area data were normalized using the MinMax normalization method, with values scaled between 0 and 1. Percentage changes in soil moisture content were then computed by calculating the variance between successive values, dividing this variance by the initial soil moisture content value, and multiplying by 100.

3. Results

3.1. Estimated leaf area index

To verify the accuracy of the LAI estimated using the EVI-based model, we employed *in-situ* LAI measurements collected in BFNP, as described in Section 2.2.1. The LAI retrieved using the EVI-based model showed a moderate relationship with in situ LAI measurements based on linear regression analysis ($R^2 = 0.52$, RMSE = 0.87) (Fig. 3).

3.2. Temporal percentage changes in net primary productivity (NPP)

The analysis of NPP changes across the study area provides a comprehensive view of its dynamic fluctuations over time. The NPP products for the period 2016–2020, as depicted in the Supplementary Material Fig. S3, highlight significant variations in NPP across the years under review. The highest mean NPP was recorded in August 2016, marking a period of relatively high productivity across the entire study area. In contrast, August 2018 witnessed the lowest NPP values, with the southern part of the BFNP experiencing the most dramatic decline. This area recorded a staggering 50% reduction in NPP compared to 2016, underscoring a critical shift in vegetation productivity Fig. 4.

A consistent decreasing trend emerges across the study area over the five-year period. NPP reductions ranged from approximately −25% to −50% annually, with the most pronounced changes concentrated in the southern region. These trends, captured in the NPP change maps (Fig. 4), visually illustrate the progressive decline, emphasizing the broader implications for ecosystem productivity and health.

3.3. Temporal variation of net primary productivity in infested and healthy spruce stands

A comparative time series of NPP between healthy stands unaffected by bark beetle infestation and infested stands is presented in Fig. 5. As evident from Figs. 5 and 4 in the Supplementary Material, NPP values in the bark beetle-infested stands were significantly lower ($\rho \leq 0.05$) compared to the NPP in the healthy stands. Specifically, in 2016, the mean NPP for healthy stands was approximately 0.14 kgC/m^2, while for infested stands, it was 0.11 kgC/m^2. Both experienced a decrease in 2018, with healthy stands dropping to 0.1 kgC/m^2 and infested stands to 0.08 kgC/m^2.

The lowest NPP was observed in 2018 for both categories. Following this, a modest recovery in NPP occurred in 2019, reaching approximately 0.12 kgC/m^2 for healthy stands and 0.09 kgC/m^2 for infested stands. By 2020, the NPP in healthy stands was approximately 0.12 kgC/m^2, reflecting a reduction of about 0.02 kgC/m^2 compared to 2016. Similarly, the NPP in infested stands declined by about 0.02 kgC/m^2 over the same period.

3.4. Temporal variation of land surface temperature in healthy and infested spruce stands

To explore the changes in LST over time between healthy and bark beetle-infested stands, we analyzed temporal trends using line charts for each of the five years covered in this study. The outcomes presented in Fig. 6 and Fig. S5 in the Supplementary Material indicate that LST values in infested stands consistently exceeded those in healthy stands across all years. This trend is particularly pronounced in the earlier years of the study (2016–2017), where the difference in LST between infested and healthy stands is significantly difference. In these years, the median LST for infested stands approaches 30 °C, while the median LST for healthy stands

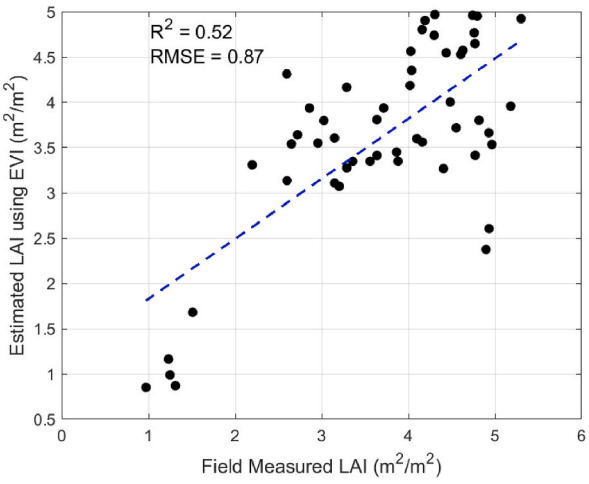

Fig. 3. Linear regression between in situ LAI measurements and LAI estimates derived from the EVI-based model over the Bavarian Forest National Park in June 2017.

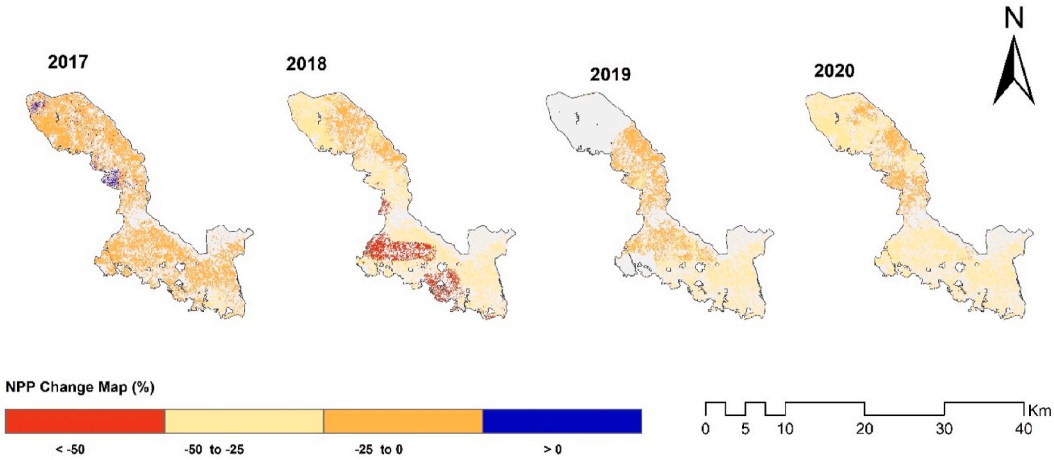

Fig. 4. Net Primary Productivity (NPP) percentage change maps during 2016–2020 for Bavarian Forest National Park in Germany. The numbers on the map represent the percentage change in Net Primary Productivity (NPP) for each year (2017–2020) relative to the reference year 2016 (set as 100%). Areas with positive values indicate an increase in NPP compared to 2016, while negative values represent a decrease.

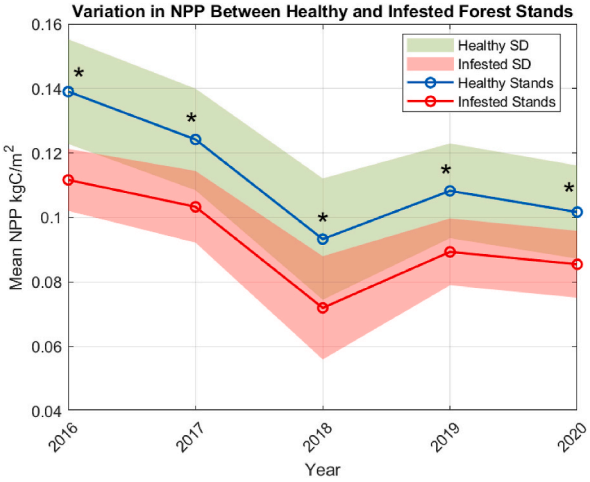

Fig. 5. Temporal variation in net primary productivity (NPP) between 2016 and 2020 for healthy and infested stands in the Bavarian Forest National Park, Germany. The year 2016 marks the start of bark beetle infestation, and the locations of infested stands from this year were used to extract NPP values for comparison in subsequent years. A similar approach was applied for infestations that began in 2017, 2018, and 2019 (see Fig. S4 in the supplementary Material). The shaded areas represent the standard deviation (SD) of NPP for healthy and infested stands, and asterisks indicate significant differences between the two groups.

remains around 25 °C. The interquartile ranges also indicate greater variability in LST values for infested stands compared to healthy stands. As the years progress from 2018 to 2020, the overall LST for infested and healthy stands shows a declining trend. However, infested stands exhibit higher LST values than healthy stands, though the difference becomes less pronounced over time. By 2020, the median LST for infested stands has decreased to approximately 25 °C, while the median LST for healthy stands has dropped to around 20 °C.

3.5. Influence of european spruce bark beetle outbreaks on net primary productivity

Next, we investigated the relationship between the bark beetle infestation area and NPP across BFNP by initially calculating the cumulative infested area (in ha) attributed to bark beetle presence for each year (Fig. S6 in supplementary Material). Fig. S6 indicates that the lowest infestation coverage (0.5 ha) was documented in 2015, while the highest coverage was observed in 2020 (6.3 ha).

Fig. 7 confirms a significant negative correlation ($r = -0.48$) between NPP values and bark beetle infestation. As the bark beetle outbreak intensified and covered more areas, there was a noticeable reduction in NPP. For example, in 2020, when 6.3 ha of the forested area within BFNP were infested, the mean NPP dropped to 0.08 KgC/m^2.

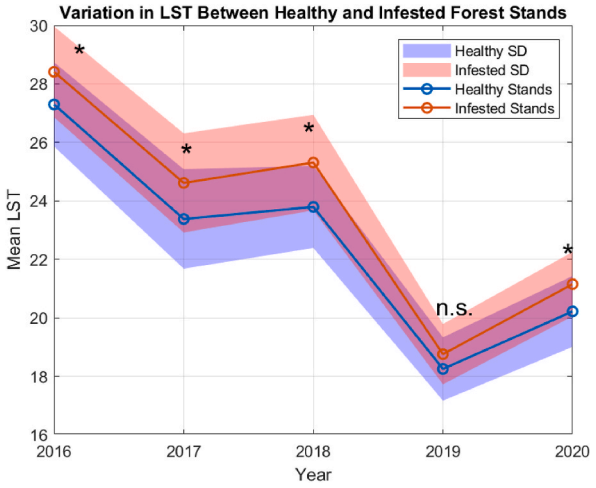

Fig. 6. Temporal variation in land surface temperature (LST) between 2016 and 2020 for healthy and infested stands in the Bavarian Forest National Park, Germany. The year 2016 marks the start of bark beetle infestation, and the locations of infested stands from this year were used to extract LST values for comparison in subsequent years. A similar approach was applied for infestations that began in 2017, 2018, and 2019 (see Fig. S5 in supplementary Material). The shaded areas represent the standard deviation (SD) of LST for healthy and infested stands, with asterisks indicating significant differences and "n.s." denoting non-significant differences.

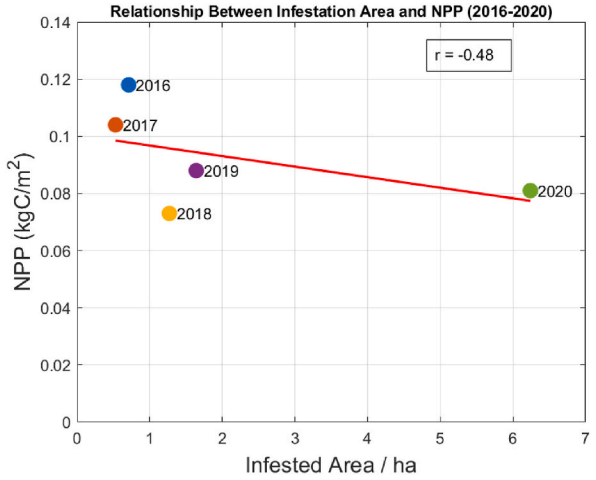

Fig. 7. Correlation between total infested area (ha) by bark beetles during 2016–2020 and mean net primary productivity (NPP) in Bavarian Forest National Park in Germany.

3.6. Temporal variation of soil moisture content and its impact on spruce-bark beetle outbreak

The monthly mean summertime soil moisture content exhibited fluctuations over the course of the five-year study (i.e., 2016–2020). The highest soil moisture content levels were observed during the summer of 2016, whereas the lowest levels were recorded in 2018. Though a relatively short time frame, Fig. 8 shows a pattern of elevated and reduced soil moisture content being succeeded by spikes in the bark beetle infestation. Moreover, this spike in infestation persisted for two to three years following periods of notably low soil moisture content (i.e., 2018). As illustrated in Fig. 8, in 2018, the soil moisture content decreased by 47% compared to the levels recorded in 2016. Subsequent to this decrease, there was an increase in bark beetle outbreaks from 13% in 2018 to 81% in 2020. In other words, the most significant increase in bark beetle outbreaks was observed two years after recording the lowest soil moisture content.

4. Discussion

This study estimated NPP by integrating high-resolution (20 m) Sentinel-2-derived LAI products with dynamic simulations using the process-based forest stand simulator LPJ-GUESS. This marks the first attempt to model NPP at such a detailed spatial scale,

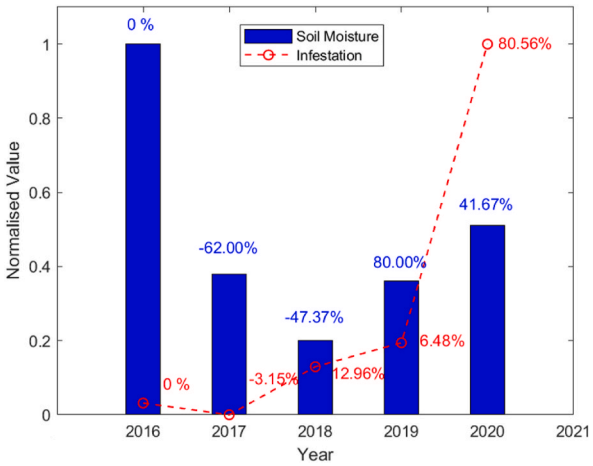

Fig. 8. Temporal changes (%) in soil moisture content and bark beetle infestation during 2016–2020 in Bavarian Forest National Park in Germany. Normalized values of soil moisture (blue bars) and infestation (red dashed line with markers) from 2016 to 2020. Percentage changes are calculated relative to the reference year 2016, where values were normalized to 1.0 for soil moisture and 0% for infestation. Positive values indicate increases, while negative values indicate decreases relative to the reference year.

overcoming the limitations of traditional coarse-resolution products like MODIS (1 km) and LPJ-GUESS (~10–50 km). The improved spatial resolution enables a more precise assessment of fine-scale forest disturbances, including bark beetle infestations and climate-induced stressors, thereby enhancing our ability to detect localized variations in forest productivity (Fig. S7). This advancement is particularly crucial in evaluating the impacts of environmental stressors on forest dynamics, as it provides a more detailed representation of ecosystem changes at a finer scale.

Forest disturbances, particularly tree mortality caused by bark beetle infestations, significantly disrupt ecosystem structure and function, affecting carbon cycling (Kurz et al., 2008; Seidl et al., 2011). Our findings align with previous studies demonstrating a sharp decline in NPP following tree mortality events (Harmon and Bell, 2020; Stephenson et al., 2011). It is important to note that while tree mortality typically leads to NPP reductions, other factors can contribute to fluctuations in NPP over time. The observed increase in NPP after 2018 (Fig. 6 and S4), despite continued bark beetle infestations in 2019 and 2020, suggests that changes in climatic conditions, shifts in vegetation productivity, or variations in forest stand composition may have influenced NPP dynamics. This temporal trend highlights the complex interactions between infestation events, environmental conditions, and NPP variability (Kretchun et al., 2016; Müller et al., 2008). Additionally, our results revealed a negative correlation between NPP and the spatial extent of infestation (Fig. 7), with larger infested areas corresponding to lower NPP values. The highest infestation area was recorded in 2020, two years after the severe 2018 drought. This aligns with Vicente-Serrano et al. (2020), who reported that the ecological impacts of drought events often persist for multiple years. Given that drought is a primary driver of European bark beetle outbreaks (Pirtskhalava-Karpova et al., 2024; Seidl et al., 2016), the extensive infestation observed in 2020 likely resulted from the delayed effects of the 2018 drought.

Moreover, the enhanced spatial resolution of NPP products plays a critical role in capturing the intricate relationships between environmental stressors, such as bark beetle infestations and climate extremes, and forest productivity. LST, in particular, influences key physiological processes, including canopy surface temperature, stomatal conductance, and the partitioning of heat fluxes between sensible (warming) and latent (cooling) heat (Abdullah et al., 2019b; Dai et al., 2004; Wehr and Saleska, 2021). In this study, we assume that LST variations due to climate change-induced extreme events, such as droughts and heatwaves, create more favourable conditions for bark beetle infestations (Rouault et al., 2006), leading to increased tree mortality and subsequent reductions in NPP. Further supporting this hypothesis, our findings indicate that NPP reached its lowest point in 2018, coinciding with minimal soil moisture content (Fig. 8). This is consistent with George et al. (2021), who found strong correlations between MODIS-NPP products and soil moisture availability. The elevated LST in 2018, which served as a proxy for the extreme heatwave, further explains the observed NPP decline. Additionally, LST was significantly higher in bark beetle-infested areas compared to unaffected Norway spruce stands (Fig. 6 and S5). This discrepancy can be attributed to canopy cover loss, which reduces shading and increases solar heating of the forest floor. Furthermore, infested trees exhibit lower stomatal conductance, reducing transpiration and diminishing latent heat flux-driven cooling (Abdullah et al., 2019b). Consequently, sensible heat retention within the canopy layer increases, further elevating LST. Our findings align with Barta et al. (2022), who reported a positive relationship between rising temperatures and tree mortality due to bark beetle infestations, alongside significant regional reductions in NPP (Allen et al., 2010).

The link between drought events and NPP reductions has been observed in various forested ecosystems worldwide. A recent study by Yin et al. (2024) found that drought events accounted for more than half of the NPP reductions in affected tropical and subtropical forests in China. This parallels our observation that minimum NPP in 2018 coincided with an intense drought event. These findings emphasize the substantial impact of drought and subsequent bark beetle infestations on forest NPP, although other factors also contribute to productivity fluctuations. As an essential climate variable (Bayat et al., 2021), LST serves as a proxy for soil moisture (Cammalleri and Vogt, 2015) and an indicator of heatwave and drought conditions (Albright et al., 2011). Our study revealed a sharp

decline in soil moisture content in the study area, with the lowest levels occurring during the extreme drought and heatwave events of 2018. This observation aligns with Sun and Pinker (2004), who demonstrated that reduced soil moisture leads to increased LST. These results underscore the importance of remotely sensed LST products in assessing the impacts of extreme climate events on forest productivity, particularly in regions with limited meteorological data.

This research provides new insights into how bark beetle infestations—one of the major threats to Norway spruce forests in Europe—interact with LST and NPP. Our findings highlight the intricate relationships between climate-induced stressors, forest health, and productivity, with broader implications for biodiversity loss and ecosystem stability. Despite these contributions, several limitations should be considered. First, the study's five-year analysis period (2016–2020) may not fully capture seasonal or intra-annual variations in NPP and bark beetle infestation dynamics. Additionally, differences in spatial resolution among the input datasets introduce potential uncertainties. For example, despite pre-processing efforts, minor misalignments between LST, soil moisture, and bark beetle infestation pixels may persist, potentially affecting the precision of spatial analyses. In addition, uncertainties also exist in the NPP estimation process, particularly regarding the LPJ-GUESS model's parameterization and its reliance on coarse-resolution environmental data. While our integration of Sentinel-2-derived LAI products with LPJ-GUESS outputs significantly improved spatial resolution and provided more detailed information (Fig. S7), incorporating additional Earth Observation (EO) datasets, such as high-resolution soil moisture and temperature products, could further enhance model accuracy. Future research should focus on refining forest models by integrating diverse EO datasets to better capture forest dynamics and reduce uncertainties in NPP estimation. Additionally, comprehensive validation against independent field measurements across diverse forest types and environmental conditions would strengthen confidence in our results. These efforts would not only improve the model's predictive capability but also provide deeper insights into the interplay between environmental stressors and forest health.

5. Conclusion

This study significantly advances NPP estimation by integrating high-resolution LAI data from Sentinel-2 with emergent outputs from a process-based forest stand simulator, LPJ-GUESS. By achieving a substantially finer NPP resolution (20 m) compared to the original 0.01-degree resolution of LPJ-GUESS, this innovative approach enhances our ability to investigate localized ecosystem disturbances, such as bark beetle infestations, and their impact on temperate forest productivity.

Our findings provide critical insights into the complex relationships between bark beetle infestation, LST, and NPP alterations. Specifically, this study revealed that bark beetle infestations were associated with significant increases in LST and marked declines in NPP over the investigated period. These results highlight how environmental stressors, such as drought and heatwaves, amplify the impact of the bark beetle infestations, affecting forest health and productivity. The sharp reduction observed in NPP during 2018 coincided with an intense drought event, illustrating the cascading effects of climatic extremes on forest ecosystems. Furthermore, this research underscores the pivotal role of LST as an essential climate variable in monitoring forest responses to drought and heatwaves. By demonstrating the utility of remotely sensed LST and soil moisture as proxies for environmental stressors, the study provides a pathway for regional-scale analyses in areas lacking meteorological data. The observed temporal dynamics of infestation offer valuable insights into the interplay between tree mortality, regeneration, and forest productivity, emphasizing the need for long-term monitoring to fully capture these processes.

The study's findings have significant implications for forest management and conservation strategies. By providing high-resolution insights into NPP dynamics and environmental stressors, this work equips forest managers with the tools to better mitigate the impacts of bark beetle infestations and climate change-related extreme events. As demonstrated here, the integration of high-resolution remote sensing data with ecological models is crucial for advancing our understanding of forest productivity and enhancing predictive capabilities.

Moving forward, future research should aim to integrate additional EO datasets, such as high-resolution soil moisture and temperature products, to further refine model accuracy. This study thus highlights the transformative potential of combining ecological modelling with high-resolution remote sensing to address pressing ecological and climatic challenges.

CRediT authorship contribution statement

Haidi Abdullah: Writing – review & editing, Writing – original draft, Visualization, Validation, Software, Methodology, Investigation, Formal analysis, Data curation, Conceptualization. **Elnaz Neinavaz:** Writing – original draft, Methodology. **Roshanak Darvishzadeh:** Writing – review & editing, Supervision, Project administration, Conceptualization. **Margarita Huesca:** Writing – review & editing, Methodology. **Andrew K. Skidmore:** Writing – review & editing, Supervision, Project administration, Funding acquisition, Conceptualization. **Mats Lindeskog:** Writing – review & editing, Validation, Methodology, Formal analysis. **Benjamin Smith:** Writing – review & editing, Supervision, Methodology, Conceptualization. **Marco Heurich:** Writing – review & editing. **Rainer Steinbrecher:** Writing – review & editing, Validation. **Marc Paganini:** Writing – review & editing, Project administration, Funding acquisition.

Ethical statement

We admit that to the best of the authors' knowledge, this submission has no potential ethical issues.

Declaration of competing interest

The authors declare the following financial interests/personal relationships which may be considered as potential competing interests: Andrew K. Skidmore reports financial support was provided by European Space Agency. If there are other authors, they declare that they have no known competing financial interests or personal relationships that could have appeared to influence the work reported in this paper.

Acknowledgement

This research has been funded by the European Space Agency (ESA) for the EO4Diversity project (Grant agreement: 4000135771) under the Biodiversity + Precursors/ESA Flagship action. The authors would like to express their appreciation for the support received for the *in-situ* data from the Bavarian Forest National Park, the Bavarian State Forest Enterprise (*Bayerische Staatsforsten*), Neuburg Forest in Germany, and the Bavarian Forest 'Data pool initiative for the Bohemian Forest Ecosystem'. Additionally, we would like to extend our gratitude to the NASA Langley Research Center (LaRC) POWER Project, funded through the NASA Earth Science/Applied Science Program, for sharing the soil moisture data.

Appendix A. Supplementary data

Supplementary data to this article can be found online at https://doi.org/10.1016/j.rsase.2025.101499.

Data availability

The authors do not have permission to share data.

References

Abdullah, H., Darvishzadeh, R., Skidmore, A.K., Groen, T.A., Heurich, M., 2018. European spruce bark beetle (Ips typographus, L.) green attack affects foliar reflectance and biochemical properties. Int. J. Appl. Earth Obs. Geoinf. 64, 199–209.

Abdullah, H., Darvishzadeh, R., Skidmore, A.K., Heurich, M., 2019a. Sensitivity of Landsat-8 OLI and TIRS data to foliar properties of early stage bark beetle (Ips typographus, L.) infestation. Remote Sens. 11 (4), 398.

Abdullah, H., Polat, N., Bilgili, A.V., Sharef, S.H., 2020. A comparison between day and night land surface temperatures using acquired satellite thermal infrared data in a winter wheat field. Remote Sens. Appl.: Society and Environment 19, 100368.

Abdullah, H., Skidmore, A.K., Darvishzadeh, R., Heurich, M., 2019b. Sentinel-2 accurately maps green-attack stage of European spruce bark beetle (Ips typographus, L.) compared with Landsat-8. Remote Sensing in Ecology and Conservation 5 (1), 87–106. https://doi.org/10.1002/rse2.93.

Ainsworth, E.A., Yendrek, C.R., Sitch, S., Collins, W.J., Emberson, L.D., 2012. The effects of tropospheric ozone on net primary productivity and implications for climate change. Annu. Rev. Plant Biol. 63, 637–661.

Albright, T.P., Pidgeon, A.M., Rittenhouse, C.D., Clayton, M.K., Flather, C.H., Culbert, P.D., Radeloff, V.C., 2011. Heat waves measured with MODIS land surface temperature data predict changes in avian community structure. Rem. Sens. Environ. 115 (1), 245–254.

Allen, C.D., Macalady, A.K., Chenchouni, H., Bachelet, D., McDowell, N., Vennetier, M., Kitzberger, T., Rigling, A., Breshears, D.D., Hogg, E.T., 2010. A global overview of drought and heat-induced tree mortality reveals emerging climate change risks for forests. For. Ecol. Manag. 259 (4), 660–684.

Anderegg, W.R., Trugman, A.T., Badgley, G., Anderson, C.M., Bartuska, A., Ciais, P., Cullenward, D., Field, C.B., Freeman, J., Goetz, S.J., 2020. Climate-driven risks to the climate mitigation potential of forests. Science 368 (6497), eaaz7005.

Ballabio, C., Lugato, E., Fernández-Ugalde, O., Orgiazzi, A., Jones, A., Borrelli, P., Montanarella, L., Panagos, P., 2019. Mapping LUCAS topsoil chemical properties at European scale using Gaussian process regression. Geoderma 355, 113912.

Barta, K.A., Hais, M., Heurich, M., 2022. Characterizing forest disturbance and recovery with thermal trajectories derived from Landsat time series data. Rem. Sens. Environ. 282, 113274.

Bayat, B., Camacho, F., Nickeson, J., Cosh, M., Bolten, J., Vereecken, H., Montzka, C., 2021. Toward operational validation systems for global satellite-based terrestrial essential climate variables. Int. J. Appl. Earth Obs. Geoinf. 95, 102240.

Berry, J., Bjorkman, O., 1980. Photosynthetic response and adaptation to temperature in higher plants. Annu. Rev. Plant Physiol. 31 (1), 491–543.

Beudert, B., Gietl, G., 2015. Long-term Monitoring in the Große Ohe Catchment, 21. Bavarian Forest National Park. Silva Gabreta.

Boegh, E., Soegaard, H., Broge, N., Hasager, C., Jensen, N., Schelde, K., Thomsen, A., 2002. Airborne multispectral data for quantifying leaf area index, nitrogen concentration, and photosynthetic efficiency in agriculture. Rem. Sens. Environ. 81 (2–3), 179–193.

Böhm, R., Auer, I., Brunetti, M., Maugeri, M., Nanni, T., Schöner, W., 2001. Regional temperature variability in the European Alps: 1760–1998 from homogenized instrumental time series. Int. J. Climatol.: A Journal of the Royal Meteorological Society 21 (14), 1779–1801.

Cammalleri, C., Vogt, J., 2015. On the role of land surface temperature as proxy of soil moisture status for drought monitoring in Europe. Remote Sens. 7 (12), 16849–16864.

Chen, J.M., Black, T., 1992. Defining leaf area index for non-flat leaves. Plant Cell Environ. 15 (4), 421–429.

Christiansen, E., Bakke, A., 1988. The spruce bark beetle of Eurasia. In: Dynamics of Forest Insect Populations: Patterns, Causes, Implications. Springer, pp. 479–503.

Cooper, L.A., Ballantyne, A.P., Holden, Z.A., Landguth, E.L., 2017. Disturbance impacts on land surface temperature and gross primary productivity in the western United States. J. Geophys. Res.: Biogeosciences 122 (4), 930–946.

Crabtree, R., Potter, C., Mullen, R., Sheldon, J., Huang, S., Harmsen, J., Rodman, A., Jean, C., 2009. A modeling and spatio-temporal analysis framework for monitoring environmental change using NPP as an ecosystem indicator. Rem. Sens. Environ. 113 (7), 1486–1496.

Dai, Y., Dickinson, R.E., Wang, Y.-P., 2004. A two-big-leaf model for canopy temperature, photosynthesis, and stomatal conductance. J. Clim. 17 (12), 2281–2299.

Das, R., Chaturvedi, R.K., Roy, A., Karmakar, S., Ghosh, S., 2023. Warming inhibits increases in vegetation net primary productivity despite greening in India. Sci. Rep. 13 (1), 21309.

Fahse, L., Heurich, M., 2011. Simulation and analysis of outbreaks of bark beetle infestations and their management at the stand level. Ecol. Model. 222 (11), 1833–1846.

Fisher, R.A., Koven, C.D., Anderegg, W.R., Christoffersen, B.O., Dietze, M.C., Farrior, C.E., Holm, J.A., Hurtt, G.C., Knox, R.G., Lawrence, P.J., 2018. Vegetation demographics in Earth System Models: a review of progress and priorities. Glob. Change Biol. 24 (1), 35–54.
Gara, T.W., Darvishzadeh, R., Skidmore, A.K., Wang, T., Heurich, M., 2019. Accurate modelling of canopy traits from seasonal Sentinel-2 imagery based on the vertical distribution of leaf traits. ISPRS J. Photogrammetry Remote Sens. 157, 108–123.
George, J.-P., Neumann, M., Vogt, J., Cammalleri, C., Lang, M., 2021. Assessing effects of drought on tree mortality and productivity in European forests across two decades: a conceptual framework and preliminary results. IOP Conf. Ser. Earth Environ. Sci.
Ghalambor, C.K., McKay, J.K., Carroll, S.P., Reznick, D.N., 2007. Adaptive versus non-adaptive phenotypic plasticity and the potential for contemporary adaptation in new environments. Funct. Ecol. 21 (3), 394–407.
Harmon, M.E., Bell, D.M., 2020. Mortality in forested ecosystems: suggested conceptual advances. Forests 11 (5), 572.
Heurich, M., Beudert, B., Rall, H., Křenová, Z., 2010. National parks as model regions for interdisciplinary long-term ecological research: the Bavarian Forest and Šumavá National Parks underway to transboundary ecosystem research. Long-term ecological research: Between theory and application 327–344.
Heurich, M., Ochs, T., Andresen, T., Schneider, T., 2013. Object-orientated image analysis for the semi-automatic detection of dead trees following a spruce bark beetle (Ips typographus) outbreak. Eur. J. For. Res. 129, 313–324. https://doi.org/10.1007/s10342-009-0331-1.
Hlásny, T., König, L., Krokene, P., Lindner, M., Montagné-Huck, C., Müller, J., Qin, H., Raffa, K.F., Schelhaas, M.-J., Svoboda, M., 2021. Bark beetle outbreaks in Europe: state of knowledge and ways forward for management. Current Forestry Reports 7, 138–165.
Jönsson, A.M., Lagergren, F., Smith, B., 2015. Forest management facing climate change-an ecosystem model analysis of adaptation strategies. Mitig. Adapt. Strategies Glob. Change 20, 201–220.
König, S., Thonfeld, F., Förster, M., Dubovyk, O., Heurich, M., 2023. Assessing combinations of Landsat, Sentinel-2 and Sentinel-1 time series for detecting bark beetle infestations. GIScience Remote Sens. 60 (1), 2226515.
Kramer, P.J., Boyer, J.S., 1995. Water Relations of Plants and Soils. Academic press.
Kretchun, A.M., Loudermilk, E.L., Scheller, R.M., Hurteau, M.D., Belmecheri, S., 2016. Climate and bark beetle effects on forest productivity—linking dendroecology with forest landscape modeling. Can. J. For. Res. 46 (8), 1026–1034.
Kurz, W.A., Dymond, C., Stinson, G., Rampley, G., Neilson, E., Carroll, A., Ebata, T., Safranyik, L., 2008. Mountain pine beetle and forest carbon feedback to climate change. Nature 452 (7190), 987–990.
Latifi, H., Holzwarth, S., Skidmore, A., Brůna, J., Červenka, J., Darvishzadeh, R., Hais, M., Heiden, U., Homolová, L., Krzystek, P., 2021. A laboratory for conceiving Essential Biodiversity Variables (EBVs)—the 'data pool initiative for the bohemian forest ecosystem'. Methods Ecol. Evol. 12 (11), 2073–2083.
Lindeskog, M., Lagergren, F., Smith, B., Rammig, A., 2021. Accounting for forest management in the estimation of forest carbon balance using the dynamic vegetation model LPJ-GUESS (v4. 0, r9333): implementation and evaluation of simulations for Europe. Geosci. Model Dev. Discuss. (GMDD) 2021, 1–42.
Marini, L., Økland, B., Jönsson, A.M., Bentz, B., Carroll, A., Forster, B., Grégoire, J.C., Hurling, R., Nageleisen, L.M., Netherer, S., 2017. Climate drivers of bark beetle outbreak dynamics in Norway spruce forests. Ecography 40 (12), 1426–1435.
Medvigy, D., Wofsy, S., Munger, J., Hollinger, D., Moorcroft, P., 2009. Mechanistic scaling of ecosystem function and dynamics in space and time: ecosystem Demography model version 2. J. Geophys. Res.: Biogeosciences 114 (G1).
Melegari, S., 2022. *Information needs on raw material supply: Assessing forest damage and disturbance* Vienna. https://www.eos-oes.eu/en/sawmill_industry_annual_reports.php.
Müller, J., Bußler, H., Goßner, M., Rettelbach, T., Duelli, P., 2008. The European spruce bark beetle Ips typographus in a national park: from pest to keystone species. Biodivers. Conserv. 17, 2979–3001.
Neinavaz, E., Darvishzadeh, R., Skidmore, A.K., Abdullah, H., 2019. Integration of Landsat-8 thermal and visible-short wave infrared data for improving prediction accuracy of forest leaf area index. Remote Sens. 11 (4), 390.
Pereira, H.M., Ferrier, S., Walters, M., Geller, G.N., Jongman, R.H., Scholes, R.J., Bruford, M.W., Brummitt, N., Butchart, S.H., Cardoso, A., 2013. Essential biodiversity variables. Science 339 (6117), 277–278.
Pfeifer, E.M., Hicke, J.A., Meddens, A.J., 2011. Observations and modeling of aboveground tree carbon stocks and fluxes following a bark beetle outbreak in the western United States. Glob. Change Biol. 17 (1), 339–350.
Pirtskhalava-Karpova, N., Trubin, A., Karpov, A., Jakuš, R., 2024. Drought initialised bark beetle outbreak in Central Europe: meteorological factors and infestation dynamic. For. Ecol. Manag. 554, 121666.
Putuhena, W.M., Cordery, I., 2000. Some hydrological effects of changing forest cover from eucalypts to Pinus radiata. Agric. For. Meteorol. 100 (1), 59–72.
Qin, Z.-H., Zhang, M.-H., Karnieli, A., Berliner, P., 2001. Mono-window algorithm for retrieving land surface temperature from Landsat TM6 data. Acta Geogr. Sin. 56 (4), 456–466.
Rouault, G., Candau, J.-N., Lieutier, F., Nageleisen, L.-M., Martin, J.-C., Warzée, N., 2006. Effects of drought and heat on forest insect populations in relation to the 2003 drought in Western Europe. Ann. For. Sci. 63 (6), 613–624.
Running, S.W., Zhao, M., 2015. Daily GPP and Annual NPP (MOD17A2/A3) Products NASA Earth Observing System MODIS Land Algorithm, 2015. MOD17 User's Guide, pp. 1–28.
Seidl, R., Müller, J., Hothorn, T., Bässler, C., Heurich, M., Kautz, M., 2016. Small beetle, large-scale drivers: how regional and landscape factors affect outbreaks of the European spruce bark beetle. J. Appl. Ecol. 53 (2), 530–540.
Seidl, R., Rammer, W., Jäger, D., Lexer, M.J., 2008. Impact of bark beetle (Ips typographus L.) disturbance on timber production and carbon sequestration in different management strategies under climate change. For. Ecol. Manag. 256 (3), 209–220.
Seidl, R., Schelhaas, M.-J., Rammer, W., Verkerk, P.J., 2014. Increasing forest disturbances in Europe and their impact on carbon storage. Nat. Clim. Change 4 (9), 806–810.
Seidl, R., Schelhaas, M.J., Lexer, M.J., 2011. Unraveling the drivers of intensifying forest disturbance regimes in Europe. Glob. Change Biol. 17 (9), 2842–2852.
Seidl, R., Thom, D., Kautz, M., Martin-Benito, D., Peltoniemi, M., Vacchiano, G., Wild, J., Ascoli, D., Petr, M., Honkaniemi, J., 2017. Forest disturbances under climate change. Nat. Clim. Change 7 (6), 395–402.
Semenza, J.C., Paz, S., 2021. Climate change and infectious disease in Europe: impact, projection and adaptation. The Lancet Regional Health–Europe 9.
Senf, C., Seidl, R., 2021. Mapping the forest disturbance regimes of Europe. Nat. Sustain. 4 (1), 63–70.
Skidmore, A.K., Coops, N.C., Neinavaz, E., Ali, A., Schaepman, M.E., Paganini, M., Kissling, W.D., Vihervaara, P., Darvishzadeh, R., Feilhauer, H., 2021. Priority list of biodiversity metrics to observe from space. Nature Ecology & Evolution 5 (7), 896–906.
Smith, B., Knorr, W., Widlowski, J.-L., Pinty, B., Gobron, N., 2008. Combining remote sensing data with process modelling to monitor boreal conifer forest carbon balances. For. Ecol. Manag. 255 (12), 3985–3994.
Smith, B., Prentice, I.C., Sykes, M.T., 2001. Representation of vegetation dynamics in the modelling of terrestrial ecosystems: comparing two contrasting approaches within European climate space. Global Ecol. Biogeogr. 621–637.
Stephenson, N.L., Van Mantgem, P.J., Bunn, A.G., Bruner, H., Harmon, M.E., O'Connell, K.B., Urban, D.L., Franklin, J.F., 2011. Causes and implications of the correlation between forest productivity and tree mortality rates. Ecol. Monogr. 81 (4), 527–555.
Sun, D., Pinker, R.T., 2004. Case study of soil moisture effect on land surface temperature retrieval. Geosci. Rem. Sens. Lett. IEEE 1 (2), 127–130.
Tait, L.W., Schiel, D.R., 2013. Impacts of temperature on primary productivity and respiration in naturally structured macroalgal assemblages. PLoS One 8 (9), e74413.
Tomes, J., Fleischer Jr, P., Kubov, M., Fleischer, P., 2024. Soil respiration after bark beetle infestation along a vertical transect in mountain spruce forest. Forests 15 (4), 611.
Wehr, R., Saleska, S.R., 2021. Calculating canopy stomatal conductance from eddy covariance measurements, in light of the energy budget closure problem. Biogeosciences 18 (1), 13–24.
Wermelinger, B., 2004. Ecology and management of the spruce bark beetle Ips typographus—a review of recent research. For. Ecol. Manag. 202 (1–3), 67–82.

Xiao, F., Ouyang, H., Fu, B., 2003. Forest ecosystem health assessment indicators and application in China. ACTA GEOGRAPHICA SINICA-CHINESE EDITION- 58 (6), 803–809.

Yin, S., Du, H., Mao, F., Li, X., Zhou, G., Xu, C., Sun, J., 2024. Spatiotemporal patterns of net primary productivity of subtropical forests in China and its response to drought. Sci. Total Environ. 913, 169439.

Yue, D., Zhou, Y., Guo, J., Chao, Z., Guo, X., 2022. Relationship between net primary productivity and soil water content in the Shule River Basin. Catena 208, 105770.

Zeppenfeld, T., Svoboda, M., DeRose, R.J., Heurich, M., Müller, J., Čížková, P., Starý, M., Bače, R., Donato, D.C., 2015. Response of mountain Picea abies forests to stand-replacing bark beetle outbreaks: neighbourhood effects lead to self-replacement. J. Appl. Ecol. 52 (5), 1402–1411.